Acta Cryst E
CRYSTALLOGRAPHIC COMMUNICATIONS

ISSN 2056-9890

Synthesis, crystal structure and thermal properties of diaquabis(4-cyanopyridine)dithiocyanatonickel(II)

Christian Näther*

Institut für Anorganische Chemie, Universität Kiel, Germany. *Correspondence e-mail: cnaether@ac.uni-kiel.de

Received 25 March 2026
Accepted 31 March 2026

Edited by W. T. A. Harrison, University of Aberdeen, United Kingdom

Keywords: synthesis; crystal structure; nickel thiocyanate; discrete aqua complex; 4-cyanopyridine; hydrogen bonding; thermal properties.

CCDC reference: 2542643

Supporting information: this article has supporting information at journals.iucr.org/e

The reaction of $Ni(NCS)_2$ and 4-cyanopyridine ($C_6H_4N_2$) in water leads to the formation of single crystals of the title compound, $[Ni(NCS)_2(C_6H_4N_2)_2(H_2O)_2]$. The asymmetric unit consists of one Ni^{II} cation, which is located on a center of inversion, as well as one thiocyanate anion, one 4-cyanopyridine coligand and one water molecule in general positions. The nickel cations therefore adopt *trans*-NiO_2N_4 octahedra, forming discrete complexes. These complexes are linked by O—H···S hydrogen bonds into layers that lie parallel to the *bc* plane. These layers are additionally linked by weak C—H···N interactions into a three-dimensional network. Powder X-ray diffraction (PXRD) indicates that an almost pure sample has been obtained. Upon heating, the title compound loses its water molecules and the 4-cyanopyridine ligands in separate steps.

1. Chemical context

Investigations on the synthesis of new coordination compounds with specific magnetic properties is still an important field in inorganic chemistry (Ferrando-Soria *et al.*, 2017). In this context, compounds in which paramagnetic metal cations are linked by small sized anionic ligands are of special importance (Yue & Gao, 2019). Numerous examples of such compounds are reported in the literature and our own work has focused on the synthesis of transition-metal thiocyanate compounds in which the cations are linked by μ-1,3-bridging anionic ligands (Wöhlert *et al.*, 2013; Werner *et al.*, 2014; Neumann *et al.*, 2018). Unfortunately, with less chalcophilic metal cations, the synthesis in solution mostly leads to compounds in which the thiocyanate anions are only terminally coordinated to the N atom.

Therefore, many years ago we developed a new route, which is based on thermal ligand removal from simple precursor complexes (Näther & Greve, 2003). We also have found that the corresponding coordination polymers with selenocyanate can be prepared by this route (Wriedt & Näther, 2010; Wöhlert *et al.*, 2012). This route is therefore one more alternative to the preparation of new coordination compounds by typical solid-state methods such as molecular milling (Braga *et al.*, 2005, 2006, James *et al.*, 2012; Do & Friščić, 2017; Stolar *et al.*, 2017) or reactions in melts (Müller-Buschbaum, 2005; Höller & Müller-Buschbaum, 2008; Zurawski *et al.*, 2012).

In view of magnetic properties, compounds based on $Co(NCS)_2$ and $Ni(NCS)_2$ are of special interest, because the former can show one-dimensional ferromagnetic ordering if they exhibit chain structures (Mautner *et al.*, 2018; Rams *et al.*, 2020), whereas the latter show three-dimensional ferromagnetic ordering if they crystallize as layered structures (Suckert *et al.*, 2016). In the course of this project, we were particularly

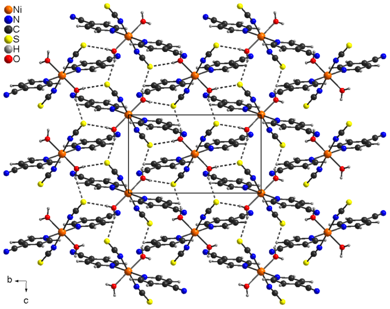

https://doi.org/10.1107/S2056989026003373

interested in pyridine derivatives as ligands and within our systematic investigations we became interested in Ni(NCS)$_2$ compounds with 4-cyanopyridine ($C_6H_4N_2$) as coligand.

With this ligand, only one Ni compound is reported: this is Ni(NCS)$_2$($C_6H_4N_2$)$_4$, which consists of discrete complexes in which the nickel cations are coordinated by two terminal N-bonded thiocyanate anions and four 4-cyanopyridine ligands, which coordinate through the pyridine N atom to the metal center (CSD refcode UBUBOL; Clegg & Harrington, 2016). In the course of our investigations, we obtained crystals of a further crystalline phase, Ni(NCS)$_2$($C_6H_4N_2$)$_2$(H_2O)$_2$ (**I**) that was identified by single crystal X-ray diffraction.

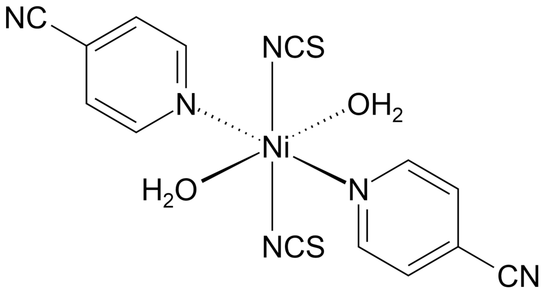

2. Structural commentary

The asymmetric unit of (**I**) is built up of one crystallographically independent nickel(II) cation that is situated on a center of inversion and one thiocyanate anion, one 4-cyanopyridine coligand and one water molecule, with all atoms located in general positions. The nickel cations are sixfold coordinated by two terminally N-bonding thiocyanate anions, two 4-cyanopyridine coligands and two water molecules into discrete complexes (Fig. 1). The 4-cyanopyridine coligand coordinates through its pyridine N atom to the metal center. The bond angles deviate slightly from the ideal values, which demonstrate that the *trans*-NiO$_2$N$_4$ octahedra are slightly distorted (Table 1).

Finally, it may be mentioned that the title compound is isotypic to one of the two modifications of Mn(NCS)$_2$($C_6H_4N_2$)$_2$(H_2O)$_2$ already reported in the literature (OJEFAN; Wellm *et al.*, 2020).

Table 1
Selected geometric parameters (Å, °).

Ni1—N1	2.035 (3)	Ni1—N11	2.108 (3)
Ni1—O1	2.084 (2)		
N1—Ni1—O1^i	87.62 (12)	N1—Ni1—N11	89.67 (13)
N1—Ni1—O1	92.38 (12)	O1—Ni1—N11	91.15 (11)
N1^i—Ni1—N11	90.32 (13)	C1—N1—Ni1	166.4 (3)

Symmetry code: (i) $-x+1, -y+1, -z+1$.

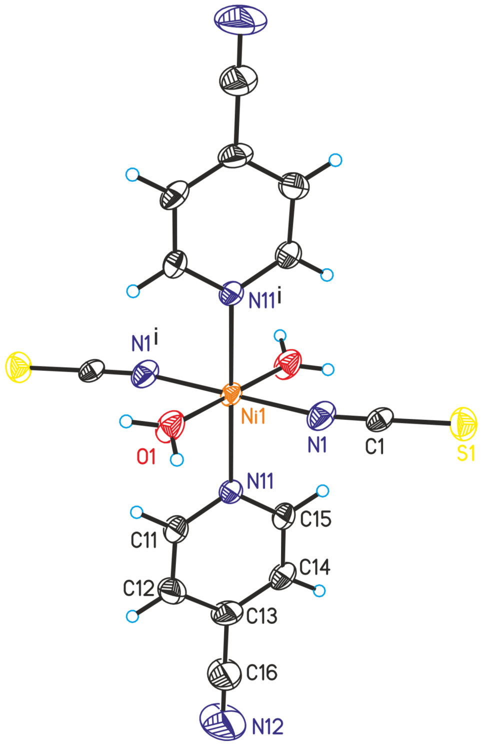

Figure 1
The molecular structure of (**I**) with labeling and displacement ellipsoids drawn at the 50% probability level. Symmetry code: (i) $-x+1, -y+1, -z+1$.

3. Supramolecular features

In the extended structure of (**I**), the complexes are linked by O—H···S hydrogen bonds between the water H atoms and the thiocyanate S atom into corrugated layers that are arranged parallel to the *bc* plane (Fig. 2). Within these layers, each S atom acts as acceptor for two hydrogen bonds from two neighboring complexes, and the H atoms of each water molecule act as donors in O—H···S hydrogen bonds to two complexes. Therefore, each complex is involved in eight hydrogen bonds to six adjacent complexes (Fig. 2). The H···S distances are relatively short and the O—H···S angles close to linear, indicating that these are relatively strong interactions (Table 2).

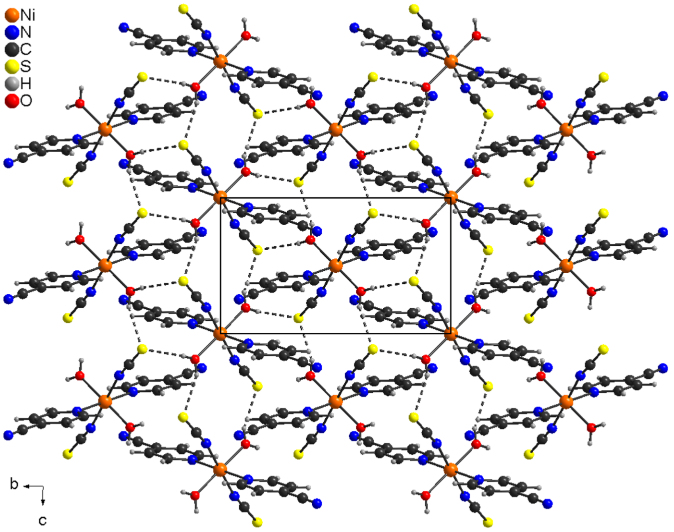

Figure 2
Crystal structure of (**I**) in a view along the crystallographic *a*-axis direction. The O—H···S hydrogen bonds are shown as dashed lines.

Table 2
Hydrogen-bond geometry (Å, °).

$D-\mathrm{H}\cdots A$	$D-\mathrm{H}$	$\mathrm{H}\cdots A$	$D\cdots A$	$D-\mathrm{H}\cdots A$
$\mathrm{O1-H1}O1\cdots \mathrm{S1}^{\mathrm{ii}}$	0.84	2.48	3.307 (3)	167
$\mathrm{O1-H2}O1\cdots \mathrm{S1}^{\mathrm{iii}}$	0.84	2.44	3.225 (3)	156
$\mathrm{C11-H11}\cdots \mathrm{N12}^{\mathrm{iv}}$	0.95	2.44	3.129 (6)	129

Symmetry codes: (ii) $-x+1, y-\frac{1}{2}, -z+\frac{3}{2}$; (iii) $-x+1, -y+1, -z+2$; (iv) $-x+2, y-\frac{1}{2}, -z+\frac{3}{2}$.

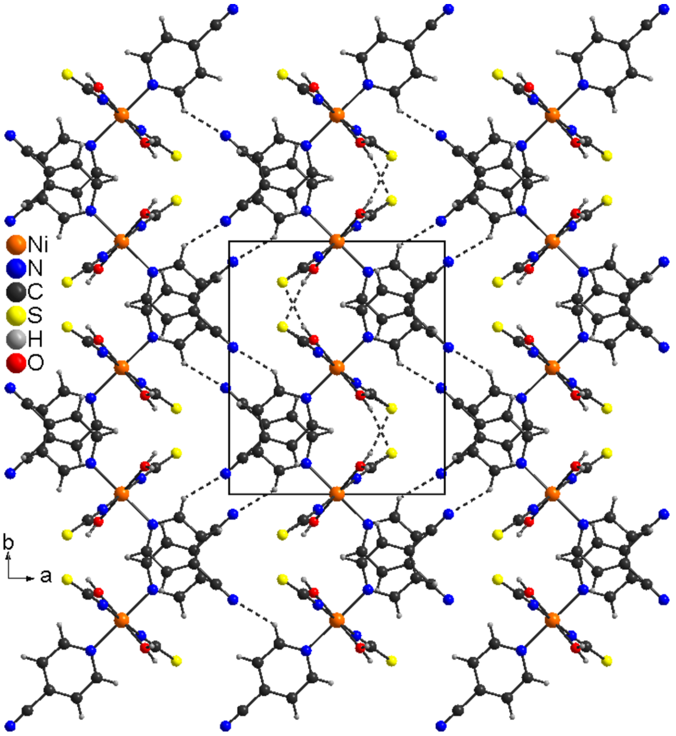

Figure 3
Crystal structure of (**I**) in a view along the crystallographic *c*-axis direction. Intermolecular $\mathrm{O-H}\cdots\mathrm{S}$ and $\mathrm{C-H}\cdots\mathrm{N}$ hydrogen bonding is shown as dashed lines.

The layers are additionally linked by pairs of centrosymmetric $\mathrm{C-H}\cdots\mathrm{N}$ interactions between the pyridine H atom and the N atom of the cyano group into a three-dimensional network (Fig. 3). The $\mathrm{C-H}\cdots\mathrm{N}$ angle is far from linear, showing that this is only a weak interaction (Table 2).

4. Additional characterization

The purity of (**I**) was investigated by X-ray powder diffraction. Comparison of the experimental powder pattern with that calculated for the title compound proves that an almost pure crystalline phase has been obtained (Fig. 4). There is a very small additional peak to the left of the most intense reflection, which indicates the presence of a very small amount of a further crystalline phase. The experimental pattern is rather noisy, which can be traced back to a low crystallinity, presumably because of grinding.

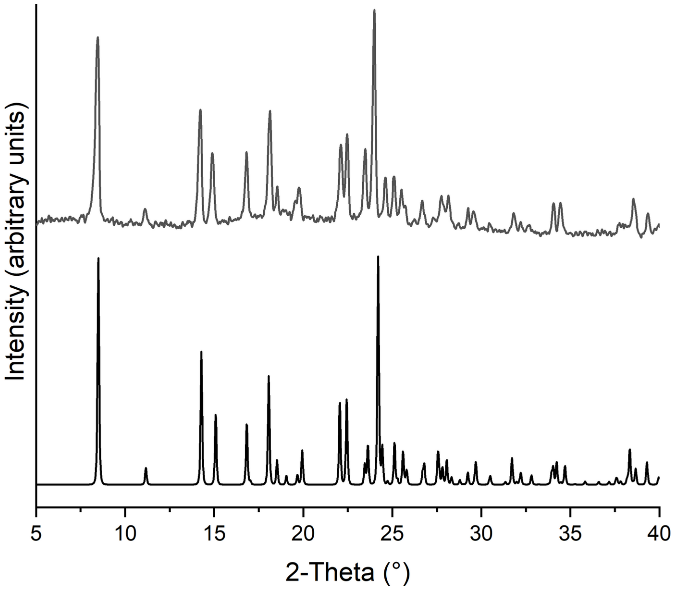

Figure 4
Experimental (top) and calculated (bottom) PXRD patterns for (**I**). Some of the reflections in the calculated pattern are slightly shifted to higher Bragg angles, which originate from the fact that the structure analysis was performed at lower temperatures.

The thermal properties of (**I**) were investigated using differential thermoanalysis coupled to thermogravimetry (DTA-TG). Upon heating, at least three mass losses are observed in the TG curve that are accompanied with endothermic events in the DTA curve (Fig. 5). The experimental mass loss in the first step of 8.5% is in good agreement with that calculated for the removal of the two water molecules of 8.1%. The DTG curve indicates that the first mass loss can be divided into two different steps, which is a hint that the two water molecules are removed in two different steps. The experimental mass losses in the second and third TG step are in good agreement with those calculated for one 4-cyanopyridine ligand in each step ($\Delta m_{\mathrm{calc.}}$ = 24.8%). This indicates

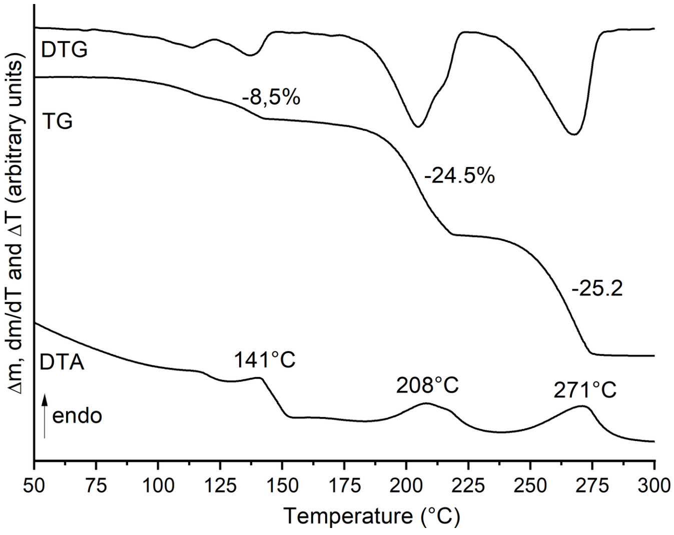

Figure 5
DTG, TG and DTA curves for (**I**). The percentage mass loss is given and the peak temperature is in °C.

that in the first TG step a compound with the composition $Ni(NCS)_2(C_6H_4N_2)_2$ is formed, which decomposes into $Ni(NCS)_2(C_6H_4N_2)$ upon further heating, before the final product of $Ni(NCS)_2$ is formed.

5. Synthesis and characterization

$Ni(NCS)_2$ was prepared from the reaction of equimolar amounts of $NiSO_4\cdot6H_2O$ with $Ba(NCS)_2\cdot3H2O$ in water. The white residue of $BaSO_4$ was filtered off and the filtrate was concentrated until complete dryness. The purity was checked by X-ray powder diffraction (XRPD). Barium thiocyanate trihydrate was purchased from Alfa Aesar and 4-cyanopyridine as well as nickel sulfate hexahydrate from Sigma-Aldrich.

1.00 mmol (174.9 mg) of $Ni(NCS)_2$ and 2.00 mmol (208.2 mg) of 4-cyanopyridine were reacted in 3 ml of water at room temperature. Within 3 d, crystals of (**I**) in the form of light-blue blocks suitable for crystal structure analysis were obtained.

Powder X-ray diffraction measurements were performed using a Stoe STADI P transmission powder diffractometer with Cu $K\alpha_1$ radiation (λ = 1.540598 Å), a Johann-type Ge(111) monochromator and a MYTHEN 1K detector from Dectris.

Thermogravimetry and differential thermoanalysis (TG–DTA) measurements were performed in a dynamic nitrogen atmosphere in Al_2O_3 crucibles with a heating rate of 4°C min^{-1} using a STA-PT 1000 thermobalance from Linseis. The TG–DTA instrument was calibrated using standard reference materials.

6. Database survey

Some more compounds with 4-cyanopyridine and transition-metal cations were found in a search of the CSD (version 5.43, last update January 2026; Groom *et al.*, 2016) using CONQUEST (Bruno *et al.*, 2002). These include $Ni(NCS)_2(C_6H_4N_2)_4$ already mentioned in the *Chemical context* section (CSD refcode UBUBOL; Clegg & Harrington, 2016).

Several compounds are reported with $Mn(NCS)_2$, including $Mn(NCS)_2(C_6H_4N_2)_4$, that also consists of discrete complexes, but which are not isotypic to $Ni(NCS)_2(C_6H_4N_2)_4$ (OJEDOZ; Wellm *et al.*, 2020). Discrete complexes with an octahedral coordination are also found in one of the two modifications of $Mn(NCS)_2(C_6H_4N_2)_2(H_2O)_2$ that is isotypic to the title compound (OJEFAN and OJEFAN01; Wellm *et al.*, 2020). Two further aqua complexes with additional 4-cyanopyridine as solvate ligand are also known (OJEFER and OJEFUH; Wellm *et al.*, 2020). Two $Mn(NCS)_2$ compounds with bridging thiocyanate anions are also reported. These include $Mn(NCS)_2(C_6H_4N_2)_2$, in which the manganese cations are octahedrally coordinated by two N- and two S-bonding thiocyanate anions and two 4-cyanopyridine ligands and are linked by pairs of anionic ligands into chains (OJEFIV; Wellm *et al.*, 2020) and $Mn(NCS)_2(C_6H_4N_2)$, in which two Mn^{II} cations are linked by pairs of thiocyanate anions into dinuclear units that are further connected by single μ-1,3-bridging anionic ligands into layers that condense into a three-dimensional network *via* the bridging 4-cyanopyridine ligands (OJEDUF and OJEDUF01; Wellm *et al.*, 2020).

With $Cu(NCS)_2$, one compound with the composition $Cu(NCS)_2(C_6H_4N_2)_2$ is also found, in which the 4-cyanopyridine coligand is only monocoordinated *via* the pyridine N atom and in which the copper cations are linked by pairs of thiocyanate anions into chains (ABOVOF; Handy *et al.*, 2017). A further solvato complex with the composition $Fe(NCS)_2(C_6H_4N_2)_2(H_2O)_2\cdot2(C_6H_4N_2)$ is also known (Jochim *et al.*, 2017).

Finally, two compounds with $Cd(NCS)_2$ are listed in the CSD, *viz*. $Cd(NCS)_2(C_6H_4N_2)_2$ (WUCLUB; Chen *et al.*, 2002), which shows the same structure as $Mn(NCS)_2(C_6H_4N_2)_2$, and $Cu(NCS)_2(C_6H_4N_2)_2$ (WUCMAI; Chen *et al.*, 2002), in which the 4-cyanopyridine ligand acts as a bridging ligand.

7. Refinement

Crystal data, data collection and structure refinement details are summarized in Table 3. The C-bound H atoms were positioned with idealized geometry and were refined with $U_{iso}(H) = 1.2U_{eq}(C)$ using a riding model. The water H atoms were located in a difference map, their bond lengths were set to standard values and finally they were refined with $U_{iso}(H) = 1.5U_{eq}(O)$ using a riding model. The crystal chosen for data collection was found to contain a small amount of at least a

Table 3
Experimental details.

Crystal data	
Chemical formula	$[Ni(NCS)_2(C_6H_4N_2)_2(H_2O)_2]$
M_r	419.13
Crystal system, space group	Monoclinic, $P2_1/c$
Temperature (K)	200
a, *b*, *c* (Å)	10.6984 (11), 12.2068 (10), 7.3974 (7)
β (°)	103.500 (12)
V (Å^3)	939.36 (16)
Z	2
Radiation type	Mo $K\alpha$
μ (mm^{-1})	1.27
Crystal size (mm)	0.13 × 0.09 × 0.06
Data collection	
Diffractometer	Stoe IPDS1
Absorption correction	Numerical (*X-SHAPE* and *X-RED32*; Stoe, 2008)
T_{min}, T_{max}	0.844, 0.899
No. of measured, independent and observed [$I > 2\sigma(I)$] reflections	5054, 1830, 1464
R_{int}	0.074
(sin $\theta/\lambda)_{max}$ (Å^{-1})	0.617
Refinement	
$R[F^2 > 2\sigma(F^2)]$, $wR(F^2)$, S	0.055, 0.150, 1.02
No. of reflections	1830
No. of parameters	115
H-atom treatment	H-atom parameters constrained
$\Delta\rho_{max}$, $\Delta\rho_{min}$ (e Å^{-3})	1.24, −1.09

Computer programs: *X-AREA* (Stoe, 2008), *SHELXT* (Sheldrick, 2015*b*), *SHELXL* (Sheldrick, 2015*a*), *DIAMOND* (Brandenburg, 1999), *XP* in *SHELXTL-PC* (Sheldrick, 2008) and *publCIF* (Westrip, 2010).

second domain, but it was not possible to index them separately to perform a twin refinement.

Acknowledgements

This work was supported by the State of Schleswig-Holstein.

References

Braga, D., Curzi, M., Grepioni, F. & Polito, M. (2005). *Chem. Commun.* pp. 2915–2917.

Braga, D., Giaffreda, S. L., Grepioni, F., Pettersen, A., Maini, L., Curzi, M. & Polito, M. (2006). *Dalton Trans.* pp. 1249–1263.

Brandenburg, K. (1999). *DIAMOND*. Crystal Impact GbR, Bonn, Germany.

Bruno, I. J., Cole, J. C., Edgington, P. R., Kessler, M., Macrae, C. F., McCabe, P., Pearson, J. & Taylor, R. (2002). *Acta Cryst.* B**58**, 389–397.

Chen, W., Liu, F. & You, X. (2002). *Bull. Chem. Soc. Jpn* **75**, 1559–1560.

Clegg, W. & Harrington, R. W. (2016). CSD Communication, Refcode UBUBOL.

Do, J. L. & Friščić, T. (2017). *ACS Cent. Sci.* **3**, 13–19.

Ferrando-Soria, J., Vallejo, J., Castellano, M., Martínez-Lillo, J., Pardo, E., Cano, J., Castro, I., Lloret, F., Ruiz-García, R. & Julve, M. (2017). *Coord. Chem. Rev.* **339**, 17–103.

Groom, C. R., Bruno, I. J., Lightfoot, M. P. & Ward, S. C. (2016). *Acta Cryst.* B**72**, 171–179.

Handy, J. V., Ayala, G. & Pike, R. D. (2017). *Inorg. Chim. Acta* **456**, 64–75.

Höller, C. J. & Müller-Buschbaum, K. (2008). *Inorg. Chem.* **47**, 10141–10149.

James, S. L., Adams, C. J., Bolm, C., Braga, D., Collier, P., Friščić, T., Grepioni, F., Harris, K. D. M., Hyett, G., Jones, W., Krebs, A., Mack, J., Maini, L., Orpen, A. G., Parkin, I. P., Shearouse, W. C., Steed, J. W. & Waddell, D. (2012). *Chem. Soc. Rev.* **41**, 413–447.

Jochim, A., Jess, I. & Näther, C. (2017). *Acta Cryst.* E**73**, 463–466.

Mautner, F. E., Traber, M., Fischer, R. C., Torvisco, A., Reichmann, K., Speed, S., Vicente, R. & Massoud, S. S. (2018). *Polyhedron* **154**, 436–442.

Müller-Buschbaum, K. (2005). *Z. Anorg. Allg. Chem.* **631**, 811–828.

Näther, C. & Greve, J. (2003). *J. Solid State Chem.* **176**, 259–265.

Neumann, T., Ceglarska, M., Germann, L. S., Rams, M., Dinnebier, R. E., Suckert, S., Jess, I. & Näther, C. (2018). *Inorg. Chem.* **57**, 3305–3314.

Rams, M., Jochim, A., Böhme, M., Lohmiller, T., Ceglarska, M., Rams, M. M., Schnegg, A., Plass, W. & Näther, C. (2020). *Chem. Eur. J.* **26**, 2837–2851.

Sheldrick, G. M. (2008). *Acta Cryst.* A**64**, 112–122.

Sheldrick, G. M. (2015*a*). *Acta Cryst.* A**71**, 3–8.

Sheldrick, G. M. (2015*b*). *Acta Cryst.* C**71**, 3–8.

Stoe (2008). *X-AREA*, *X-RED32* and *X-SHAPE*. Stoe & Cie, Darmstadt, Germany.

Stolar, T., Batzdorf, L., Lukin, S., Žilić, D., Motillo, C., Friščić, T., Emmerling, F., Halasz, I. & Užarević, K. (2017). *Inorg. Chem.* **56**, 6599–6608.

Suckert, S., Rams, M., Böhme, M., Germann, L. S., Dinnebier, R. E., Plass, W., Werner, J. & Näther, C. (2016). *Dalton Trans.* **45**, 18190–18201.

Wellm, C., Neumann, T., Gallo, G., Dziubyna, A. M., Rams, M., Dinnebier, R. E. & Näther, C. (2020). *Cryst. Growth Des.* **20**, 3374–3385.

Werner, J., Rams, M., Tomkowicz, Z. & Näther, C. (2014). *Dalton Trans.* **43**, 17333–17342.

Westrip, S. P. (2010). *J. Appl. Cryst.* **43**, 920–925.

Wöhlert, S., Ruschewitz, U. & Näther, C. (2012). *Cryst. Growth Des.* **12**, 2715–2718.

Wöhlert, S., Wriedt, M., Fic, T., Tomkowicz, Z., Haase, W. & Näther, C. (2013). *Inorg. Chem.* **52**, 1061–1068.

Wriedt, M. & Näther, C. (2010). *Chem. Commun.* **46**, 4707–4709.

Yue, G. & Gao, E. Q. (2019). *Coord. Chem. Rev.* **382**, 1–31.

Zurawski, A., Rybak, J. C., Meyer, L. V., Matthes, P. R., Stepanenko, V., Dannenbauer, N., Würthner, F. & Müller-Buschbaum, K. (2012). *Dalton Trans.* **41**, 4067–4078.

supporting information

Acta Cryst. (2026). E**82**, 441-445 [https://doi.org/10.1107/S2056989026003373]

Synthesis, crystal structure and thermal properties of diaquabis(4-cyanopyridine)dithiocyanatonickel(II)

Christian Näther

Computing details

Diaquabis(pyridine-4-carbonitrile)dithiocyanatonickel(II)

Crystal data

$[Ni(NCS)_2(C_6H_4N_2)_2(H_2O)_2]$	$F(000) = 428$
$M_r = 419.13$	$D_x = 1.482$ Mg m^{-3}
Monoclinic, $P2_1/c$	Mo $K\alpha$ radiation, $\lambda = 0.71073$ Å
$a = 10.6984$ (11) Å	Cell parameters from 6692 reflections
$b = 12.2068$ (10) Å	$\theta = 4.6$–$26.9°$
$c = 7.3974$ (7) Å	$\mu = 1.27$ mm^{-1}
$\beta = 103.500$ (12)°	$T = 200$ K
$V = 939.36$ (16) Å^3	Block, light blue
$Z = 2$	0.13 × 0.09 × 0.06 mm

Data collection

Stoe IPDS-1 diffractometer	1830 independent reflections
Phi scans	1464 reflections with $I > 2\sigma(I)$
Absorption correction: numerical (X-Shape and X-Red32; Stoe, 2008)	$R_{int} = 0.074$
$T_{min} = 0.844$, $T_{max} = 0.899$	$\theta_{max} = 26.0°$, $\theta_{min} = 2.6°$
5054 measured reflections	$h = -13 \rightarrow 12$
	$k = -13 \rightarrow 15$
	$l = -9 \rightarrow 9$

Refinement

Refinement on F^2	Primary atom site location: dual
Least-squares matrix: full	Hydrogen site location: mixed
$R[F^2 > 2\sigma(F^2)] = 0.055$	H-atom parameters constrained
$wR(F^2) = 0.150$	$w = 1/[\sigma^2(F_o^2) + (0.1103P)^2]$ where $P = (F_o^2 + 2F_c^2)/3$
$S = 1.02$	$(\Delta/\sigma)_{max} < 0.001$
1830 reflections	$\Delta\rho_{max} = 1.24$ e Å^{-3}
115 parameters	$\Delta\rho_{min} = -1.09$ e Å^{-3}
0 restraints	

Special details

Geometry. All esds (except the esd in the dihedral angle between two l.s. planes) are estimated using the full covariance matrix. The cell esds are taken into account individually in the estimation of esds in distances, angles and torsion angles; correlations between esds in cell parameters are only used when they are defined by crystal symmetry. An approximate (isotropic) treatment of cell esds is used for estimating esds involving l.s. planes.

Fractional atomic coordinates and isotropic or equivalent isotropic displacement parameters (Å^2)

	x	y	z	$U_{\rm iso}$*/$U_{\rm eq}$
Ni1	0.500000	0.500000	0.500000	0.0212 (2)
N1	0.4116 (3)	0.5615 (3)	0.6935 (4)	0.0322 (7)
C1	0.3433 (3)	0.6039 (3)	0.7731 (4)	0.0228 (7)
S1	0.24664 (9)	0.66118 (9)	0.88587 (14)	0.0356 (3)
N11	0.6437 (3)	0.6209 (2)	0.5724 (4)	0.0259 (7)
C11	0.7680 (3)	0.5930 (3)	0.6064 (6)	0.0324 (8)
H11	0.788824	0.517784	0.598705	0.039*
C12	0.8678 (4)	0.6673 (3)	0.6520 (6)	0.0384 (10)
H12	0.954934	0.644175	0.676692	0.046*
C13	0.8361 (4)	0.7766 (3)	0.6604 (6)	0.0398 (10)
C14	0.7090 (4)	0.8075 (3)	0.6257 (6)	0.0375 (9)
H14	0.686068	0.882410	0.630713	0.045*
C15	0.6155 (4)	0.7275 (3)	0.5833 (6)	0.0304 (8)
H15	0.527780	0.748690	0.561004	0.036*
C16	0.9377 (5)	0.8572 (4)	0.7069 (9)	0.0598 (15)
N12	1.0171 (5)	0.9193 (5)	0.7477 (11)	0.099 (2)
O1	0.6085 (3)	0.3904 (2)	0.6893 (4)	0.0352 (7)
H1O1	0.654313	0.339361	0.663891	0.053*
H2O1	0.639203	0.397151	0.804131	0.053*

Atomic displacement parameters (Å^2)

	U^{11}	U^{22}	U^{33}	U^{12}	U^{13}	U^{23}
Ni1	0.0251 (4)	0.0130 (3)	0.0255 (4)	0.0010 (2)	0.0063 (2)	−0.0014 (2)
N1	0.0400 (17)	0.0227 (16)	0.0361 (17)	−0.0037 (13)	0.0131 (14)	−0.0042 (13)
C1	0.0307 (17)	0.0184 (16)	0.0207 (16)	−0.0058 (13)	0.0085 (14)	−0.0014 (13)
S1	0.0338 (5)	0.0416 (6)	0.0342 (5)	0.0045 (4)	0.0135 (4)	−0.0029 (4)
N11	0.0255 (14)	0.0164 (14)	0.0342 (16)	0.0005 (11)	0.0036 (12)	−0.0023 (11)
C11	0.0315 (19)	0.0180 (17)	0.046 (2)	0.0023 (14)	0.0060 (16)	−0.0020 (16)
C12	0.0284 (18)	0.029 (2)	0.053 (2)	−0.0004 (16)	0.0007 (17)	−0.0036 (18)
C13	0.038 (2)	0.026 (2)	0.052 (2)	−0.0102 (16)	0.0027 (18)	−0.0071 (18)
C14	0.043 (2)	0.0168 (17)	0.051 (2)	0.0001 (16)	0.0069 (18)	−0.0087 (16)
C15	0.0303 (17)	0.0194 (17)	0.041 (2)	0.0030 (14)	0.0078 (15)	−0.0047 (15)
C16	0.044 (3)	0.033 (2)	0.098 (4)	−0.007 (2)	0.007 (3)	−0.012 (3)
N12	0.057 (3)	0.052 (3)	0.176 (7)	−0.028 (2)	0.003 (3)	−0.021 (4)
O1	0.0470 (16)	0.0237 (13)	0.0311 (14)	0.0093 (12)	0.0017 (12)	−0.0001 (11)

Geometric parameters (Å, º)

Ni1—N1^{i}	2.035 (3)	C11—H11	0.9500
Ni1—N1	2.035 (3)	C12—C13	1.382 (6)
Ni1—O1^{i}	2.084 (2)	C12—H12	0.9500
Ni1—O1	2.084 (2)	C13—C14	1.376 (6)
Ni1—N11^{i}	2.108 (3)	C13—C16	1.446 (6)
Ni1—N11	2.108 (3)	C14—C15	1.381 (5)

N1—C1	1.161 (5)	C14—H14	0.9500
C1—S1	1.630 (4)	C15—H15	0.9500
N11—C11	1.339 (5)	C16—N12	1.127 (6)
N11—C15	1.342 (5)	O1—H1O1	0.8400
C11—C12	1.381 (6)	O1—H2O1	0.8400

N1^{i}—Ni1—N1	180.0	N11—C11—C12	123.8 (4)
N1^{i}—Ni1—O1^{i}	92.38 (12)	N11—C11—H11	118.1
N1—Ni1—O1^{i}	87.62 (12)	C12—C11—H11	118.1
N1^{i}—Ni1—O1	87.62 (12)	C11—C12—C13	117.5 (4)
N1—Ni1—O1	92.38 (12)	C11—C12—H12	121.3
O1^{i}—Ni1—O1	180.0	C13—C12—H12	121.3
N1^{i}—Ni1—N11^{i}	89.68 (13)	C14—C13—C12	119.9 (4)
N1—Ni1—N11^{i}	90.33 (13)	C14—C13—C16	120.9 (4)
O1^{i}—Ni1—N11^{i}	91.15 (11)	C12—C13—C16	119.2 (4)
O1—Ni1—N11^{i}	88.85 (11)	C13—C14—C15	118.7 (4)
N1^{i}—Ni1—N11	90.32 (13)	C13—C14—H14	120.6
N1—Ni1—N11	89.67 (13)	C15—C14—H14	120.6
O1^{i}—Ni1—N11	88.85 (11)	N11—C15—C14	122.6 (3)
O1—Ni1—N11	91.15 (11)	N11—C15—H15	118.7
N11^{i}—Ni1—N11	180.00 (11)	C14—C15—H15	118.7
C1—N1—Ni1	166.4 (3)	N12—C16—C13	178.2 (8)
N1—C1—S1	178.9 (3)	Ni1—O1—H1O1	126.0
C11—N11—C15	117.5 (3)	Ni1—O1—H2O1	129.9
C11—N11—Ni1	120.2 (2)	H1O1—O1—H2O1	100.9
C15—N11—Ni1	122.2 (2)		

Symmetry code: (i) $-x+1$, $-y+1$, $-z+1$.

Hydrogen-bond geometry (Å, º)

D—H···*A*	*D*—H	H···*A*	*D*···*A*	*D*—H···*A*
O1—H1*O*1···S1^{ii}	0.84	2.48	3.307 (3)	167
O1—H2*O*1···S1^{iii}	0.84	2.44	3.225 (3)	156
C11—H11···N12^{iv}	0.95	2.44	3.129 (6)	129

Symmetry codes: (ii) $-x+1$, $y-1/2$, $-z+3/2$; (iii) $-x+1$, $-y+1$, $-z+2$; (iv) $-x+2$, $y-1/2$, $-z+3/2$.